JOURNAL OF GEOPHYSICAL RESEARCH, VOL. 115, B07313, doi:10.1029/2009JB006859, 2010

Coseismic velocity variations caused by static stress changes associated with the 2001 M_w = 4.3 Agios Ioanis earthquake in the Gulf of Corinth, Greece

L. Cociani,[1] C. J. Bean,[1] H. Lyon-Caen,[2] F. Pacchiani,[3] and A. Deschamps[4]

Received 9 August 2009; revised 27 November 2009; accepted 16 March 2010; published 31 July 2010.

[1] The analysis of temporal variations in the seismic velocity across faults can be used to estimate in situ stress changes. Seismic velocity of propagation depends on the fault stiffness, which is a function of stress. The coda wave interferometry technique is applied to seven families of repeating earthquakes (multiplets) recorded on the southern shore of the Gulf of Corinth, Greece, to estimate high precision velocity changes in the Earth's crust associated with the M_w = 4.3 Agios Ioanis earthquake. Results show that the Agios Ioanis event causes a perturbation in elastic properties at seismogenic depth, resulting in a reduction of 0.2% in the seismic velocity. The results are not consistent with either damage induced by dynamic stresses nor a fluid transient origin. In contrast, both the spatial distribution and magnitude of the velocity perturbation correlate well with modeled static stress variations. This suggests that the measured changes in the mechanical properties of the seismogenic crust can be attributed to a change in static stress field associated with the M_w = 4.3 Agios Ioanis earthquake. The velocity changes indicate an unclamping of the Pyrgaki fault at depth, which has local hazard implications.

Citation: Cociani, L., C. J. Bean, H. Lyon-Caen, F. Pacchiani, and A. Deschamps (2010), Coseismic velocity variations caused by static stress changes associated with the 2001 M_w = 4.3 Agios Ioanis earthquake in the Gulf of Corinth, Greece, *J. Geophys. Res.*, *115*, B07313, doi:10.1029/2009JB006859.

1. Introduction

[2] Faults and fractures play a critical role in controlling many geological and geophysical phenomena, yet a basic understanding of their fundamental in situ properties such as strength, cohesion, hydraulic conductivity, or stress state is still lacking. In particular, monitoring the evolution of stress in deep fault zones is very important for an understanding of how faults evolve through the stages of their earthquake cycles. Stress-induced changes of fault compliance can alter the effective mechanical properties of the fault zone and hence the velocity at which seismic waves pass through the medium. Recent controlled source experiments demonstrate that tidal oscillations, changes in the barometric pressure, and variations in the stress field in seismogenic areas can be successfully monitored by measuring seismic wave velocities [*Gret et al.*, 2006; *Niu et al.*, 2008; *Silver et al.*, 2007; *Yamamura et al.*, 2003a, 2003b]. However, the deep boreholes required to study active fault zones have associated high costs and logistical difficulties.

[3] A possible alternative to overcome these limitations is the use of natural repeatable sources. Stress generated by tectonic loading or by changes in fluid pressure can repeatedly be concentrated and released at the same asperities along faults and thus produces repeating earthquakes, called multiplets [e.g., *Bokelmann and Harjes*, 2000]. These events, having colocated sources and the same source mechanism, have nearly identical waveforms when recorded by the same fixed station [e.g., *Geller and Mueller*, 1980]. The precise measurement of wave traveltime delay for identical sources yields accurate estimates of the changes in the velocity of the medium in the time interval separating the events of a doublet [e.g., *Poupinet et al.*, 1984]. However, typical stress changes in rocks usually only cause small variations in velocity (a fraction of a percent). Therefore, since the direct (ballistic) arrivals only sample the stressed region once, they are not very sensitive to such small changes. Instead, waves multiply scattered in the medium are increasingly more sensitive to these small velocity changes since they repeatedly sample the same area. The coda wave interferometry (CWI) method [*Snieder*, 2006] exploits this characteristic to determine velocity changes with exquisite accuracy. The CWI technique has been successfully used to detect temperature-related nonlinear behavior of the seismic velocity in granite [*Snieder et al.*, 2002], seasonal variations in seismic velocity at Fogo

[1]Seismology and Computational Rock Physics Laboratory, School of Geological Sciences, University College Dublin, Belfield, Dublin, Ireland.
[2]Laboratoire de Géologie, Ecole Normale Supérieure, CNRS, Paris, France.
[3]Istituto Nazionale di Oceanografia e di Geofisica Sperimentale, Borgo Grotta Gigante, Sgonico, Trieste, Italy.
[4]UMR Géoazur, UNS, CNRS, IRD, OCA, Valbonne, France.

0148-0227/10/2009JB006859

volcano [*Martini et al.*, 2009], stress-related changes at Vesuvius volcano [*Pandolfi et al.*, 2006], stress changes in a mining environment [*Gret et al.*, 2006], and changes in the compliance between synthetic seismic data generated in two fractured models [*Möllhoff and Bean*, 2009]. Therefore, it is well suited for monitoring stress evolution in heterogeneous fault zones.

[4] Applying the simple concept of elastic rebound, the temporal evolution of stress state of faults follows the two main phases of the earthquake cycle: the elastic strain energy accumulation stage arising from ongoing tectonic loading and the stress release stage that follows rupture nucleation. However, modification of the stress state of a given fault can also be related to activity on neighboring faults, which may result in static ("permanent" loading) and/or dynamic (transient oscillatory waves) stress changes on the given fault.

[5] These coseismic stress changes can lead to either an increase or decrease of the applied normal and shear stresses on nearby faults, depending on their orientation with respect to the stress tensor following the coseismic event. Variations in the applied stress change the elastic moduli of rocks and render fault zones either more or less compliant, thus also affecting the seismic velocity of waves propagating across fault zones. The strain amplitudes of seismic waves can also alter the elastic modulus of fault gouge [e.g., *Johnson and Jia*, 2005]. Both static and dynamic stress changes are associated with alterations of fault properties and with an increase in seismic activity.

[6] In the near field, static changes in the stress tensor caused by coseismic deformation have been widely modeled using the Coulomb failure criterion; this can also explain the spatial distribution of the aftershocks [e.g., *King et al.*, 1994; *McCloskey and Nalbant*, 2009; *Nalbant et al.*, 1998]. In the far field, where static stress changes are considered too small to trigger earthquakes, transient stresses caused by the shaking of large-amplitude seismic waves can still trigger earthquakes [e.g., *Hill et al.*, 1993; *Johnson and Jia*, 2005; *Velasco et al.*, 2008]. In the near field, it is difficult to separate the static from the dynamic effect, as they have similar amplitudes.

[7] In order to better understand the physics of earthquake nucleation and fault interaction and to forecast earthquake probability, it is important to identify which mechanism is predominant in the near field. Hitherto, this unresolved problem has been tackled by analyzing the spatial and temporal distribution of aftershocks. However, a consensus on whether the dominant role in this process is played by permanent or transient stress changes has not been reached yet. In contrast, our approach to determine which physical mechanism dominates the process of altering the mechanical properties of a neighboring fault zone in the near field is to exploit the stress dependence of seismic wave velocity across faults. For this purpose, we study the static and dynamic effect on the neighboring fault system of a M_w = 4.3 event, the Agios Ioanis earthquake, which occurred in April 2001 in the Gulf of Corinth, Greece.

[8] In this study, we pursue two main objectives: (1) the assessment of the preseismic, coseismic, and postseismic elastic properties of the crustal volume local to the M_w = 4.3 event and (2) the determination of the main mechanism causing the observed perturbations in the medium properties. We use the CWI technique on families of repeating earthquakes to detect sudden small velocity changes of the medium caused by the Agios Ioanis event. A detailed analysis of the CWI results, combined with normal stress change calculations, are then applied to estimate the predominant mechanism causing the velocity variations in fault zones neighboring the M_w = 4.3 event.

2. Data

2.1. Dataset Description

[9] In this study, we use the microseismicity with magnitudes between 0.5 and 4.3, belonging to the 2001 sequence (Figure 1). The data were recorded by the Corinth Rift Laboratory Network (CRLNET). This network consists of 12, three-component, short-period seismometers, and seven of these are installed in boreholes 60–130 m deep. The events were located [*Lyon-Caen et al.*, 2004] using HYPO71 [*Lee and Lahr*, 1972] with a 1-D velocity model [*Rigo et al.*, 1996]. Most events appear located underneath the Pyrgaki fault zone almost directly below AIO station (Figure 1). The largest event in this sequence was the M_w = 4.3 Agios Ioanis earthquake recorded on the 8 April (Figure 2). Analysis of the seismicity rate and earthquake magnitude evolution suggests a swarm rather than a main shock-aftershock sequence [*Pacchiani and Lyon-Caen*, 2009]. This swarm is not associated with any of the main north dipping normal faults mapped at the surface, such as the Pyrgaki, Mamoussia, or Helike faults (Figure 1). The preferred fault plane solution for the M_w = 4.3 event has a strike of 220°, a dip of 40°, and a rake of −160° [*Zahradnik et al.*, 2004] in agreement with the seismicity and the relocation analysis that indicates a similarly oriented fault plane dipping NW [*Pacchiani*, 2006]. This suggests the existence of a hidden transverse fault, named the Kerinitis fault, oriented nearly perpendicular to the main normal faults of the Gulf and, most importantly, active beneath the Pyrgaki fault [*Pacchiani and Lyon-Caen*, 2009].

[10] Data mainly from station AIO were used in this work as the station was installed in limestone bedrock in a 130 m deep borehole, recording data with a high signal-to-noise ratio. In addition, we also used data from DIM station, located about 6 km north of AIO and installed in a borehole into Pliocene Gilbert-type delta conglomerates [e.g., *Giurgea et al.*, 2004]. We analyzed about 1000 events that occurred between 26 March and 18 April 2001, located in a volume of ~125 km^3, between the Pyrgaki and Keritinis faults, at a depth ranging from 5 to 10 km. The large number of events in the swarm and the frequent occurrence of multiplets make this area a natural laboratory for searching the temporal evolution of fault properties associated with the M_w = 4.3 event. In fact, we can use families of repeating events that belong to the Keritinis fault to illuminate the medium above it and measure possible changes in the effective seismic velocity caused by alterations in the mechanical properties of the Pyrgaki fault zone (Figure 1).

2.2. Extraction and Location of the Multiplets

[11] In order to facilitate the extraction of multiplets from the 2001 swarm, we band-pass filtered all data from 1 to 10 Hz, recorded at station AIO, to eliminate incoherent noise at higher frequencies. We aligned the waveforms to

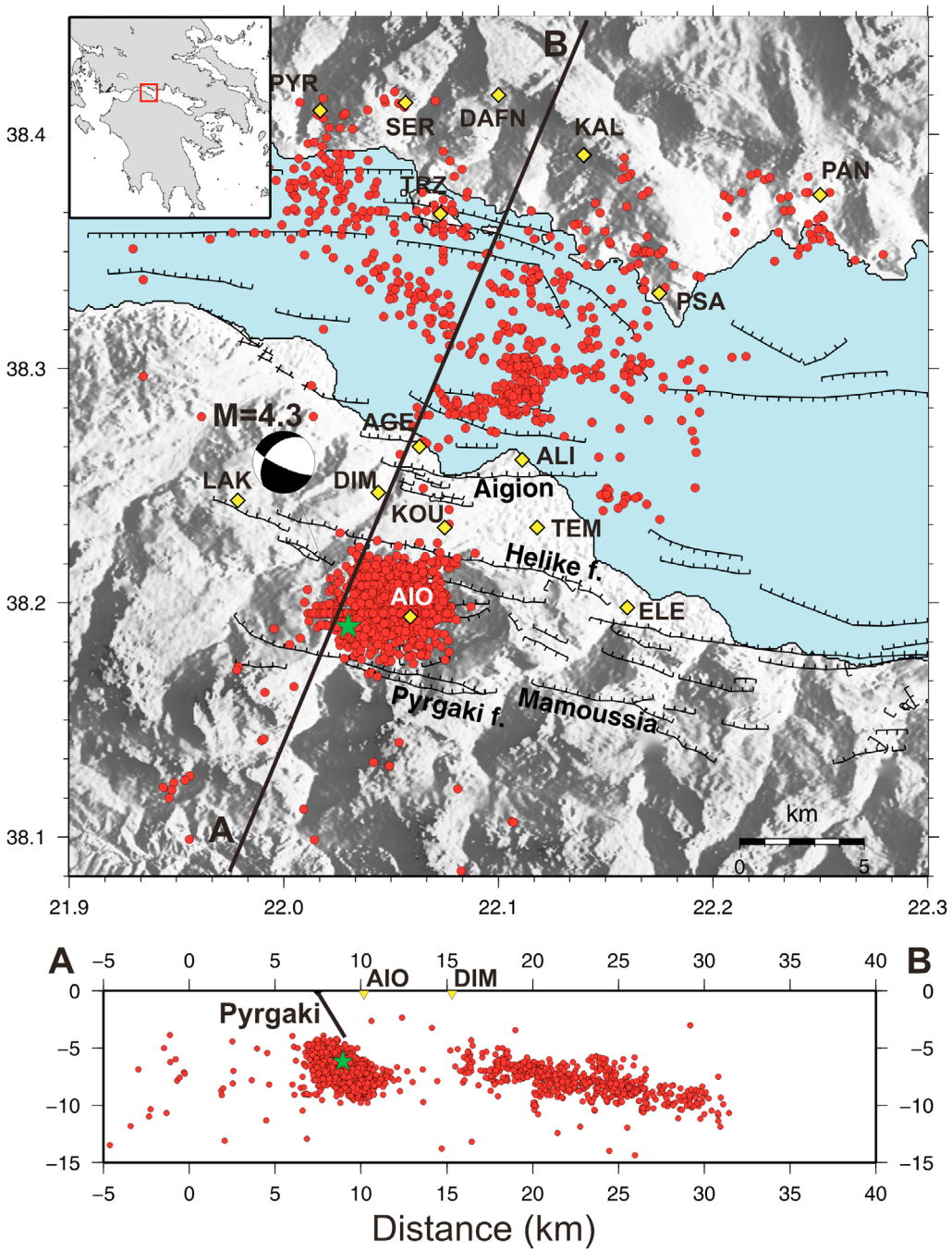

Figure 1. (top) Shaded relief map of the western Gulf of Corinth including the Corinth Rift seismological network (represented by the diamonds), the seismicity recorded in 2001 (circles; data after *Lyon-Caen et al.* [2004]), and major faults. The area related to the seismic swarm recorded in 2001 is located between the surface expression of the Pyrgaki and Helike faults. The star indicates the M_w = 4.3 Agios Ioanis epicenter location. The focal mechanism indicated normal faulting with a strong component of strike-slip motion. (bottom) Vertical cross section as indicated by the thick straight line in the map view, showing the location of the seismic swarm in relation to the Pyrgaki fault, the Agios Ioanis hypocenter, and the two main stations used in this study, AIO and DIM.

the manually picked *P* arrival and cross-correlated the seismic waveforms along a 15 s window starting 0.2 s before the first arrival time. Only multiplets with a correlation coefficient greater than 0.9 between each event pair were considered, thus defining tight clusters in which all events correlate well with each other. This resulted in 33 families of repeating earthquakes with a minimum of six events in each family. Among those, to ensure a good temporal sampling, we selected only multiplets with a minimum of two events occurring before and two events after the M_w = 4.3 event,

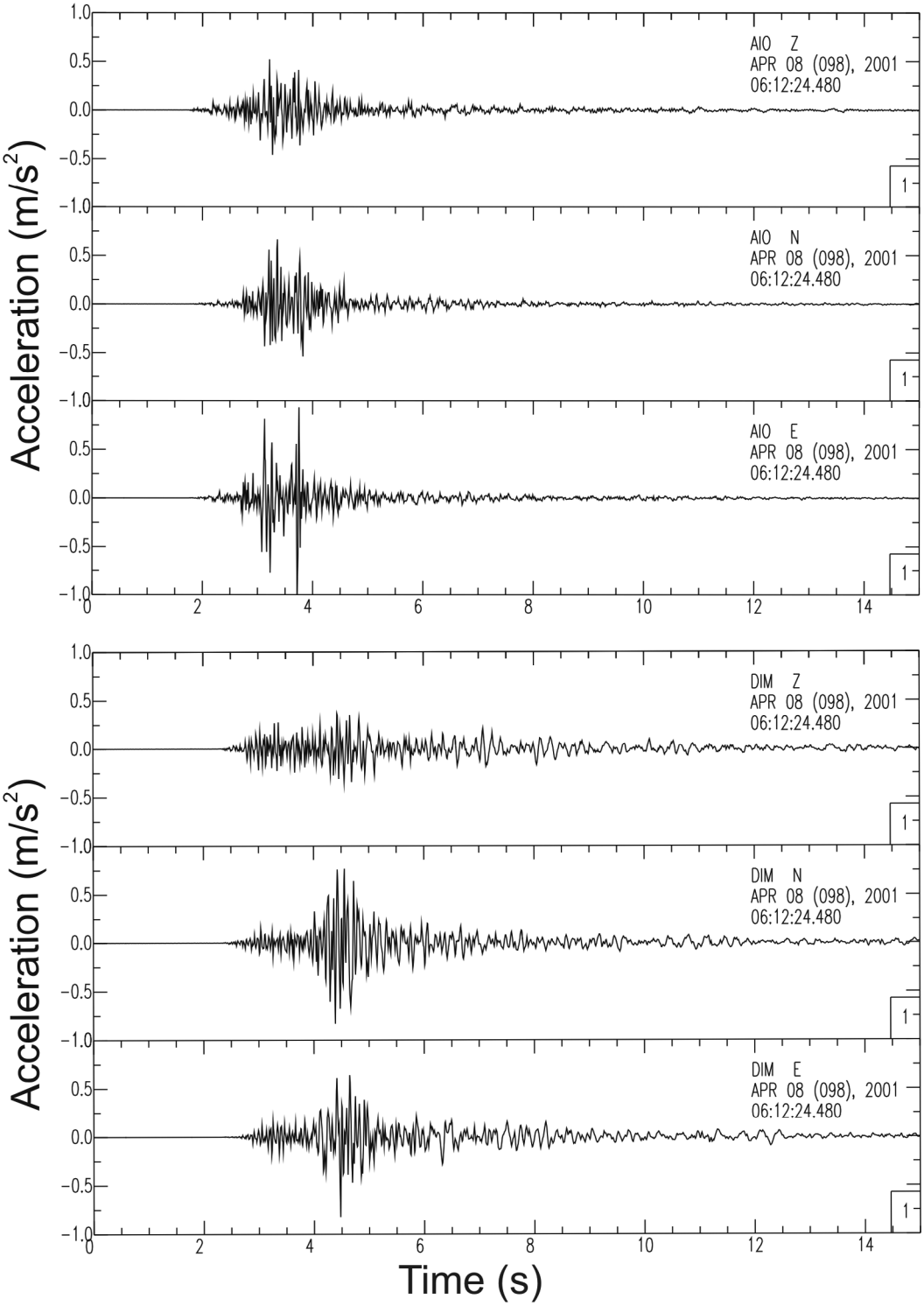

Figure 2. Three component accelerograms for the Agios Ioanis earthquake recorded at station (top) AIO and (bottom) DIM.

which reduced the number of families to 7. The choice of a high-correlation coefficient for the multiplets search ensures a high waveform coherency (Figure 3a), thus limiting differences in the source mechanism and interevent distance. In addition, we performed the same procedure using stations LAK, DIM, and TEM (Figure 1); however, we were able to identify, only at station DIM, the same multiplets recorded at station AIO, as the signal-to-noise ratio at stations LAK and TEM was poor for these events. Therefore only stations AIO and DIM are used in the velocity analysis.

[12] In order to disregard events whose source offset was greater than a quarter of the wavelength, Fresnel zone [*Geller and Mueller*, 1980], we computed the relative relocation of each of the seven multiplets using the double

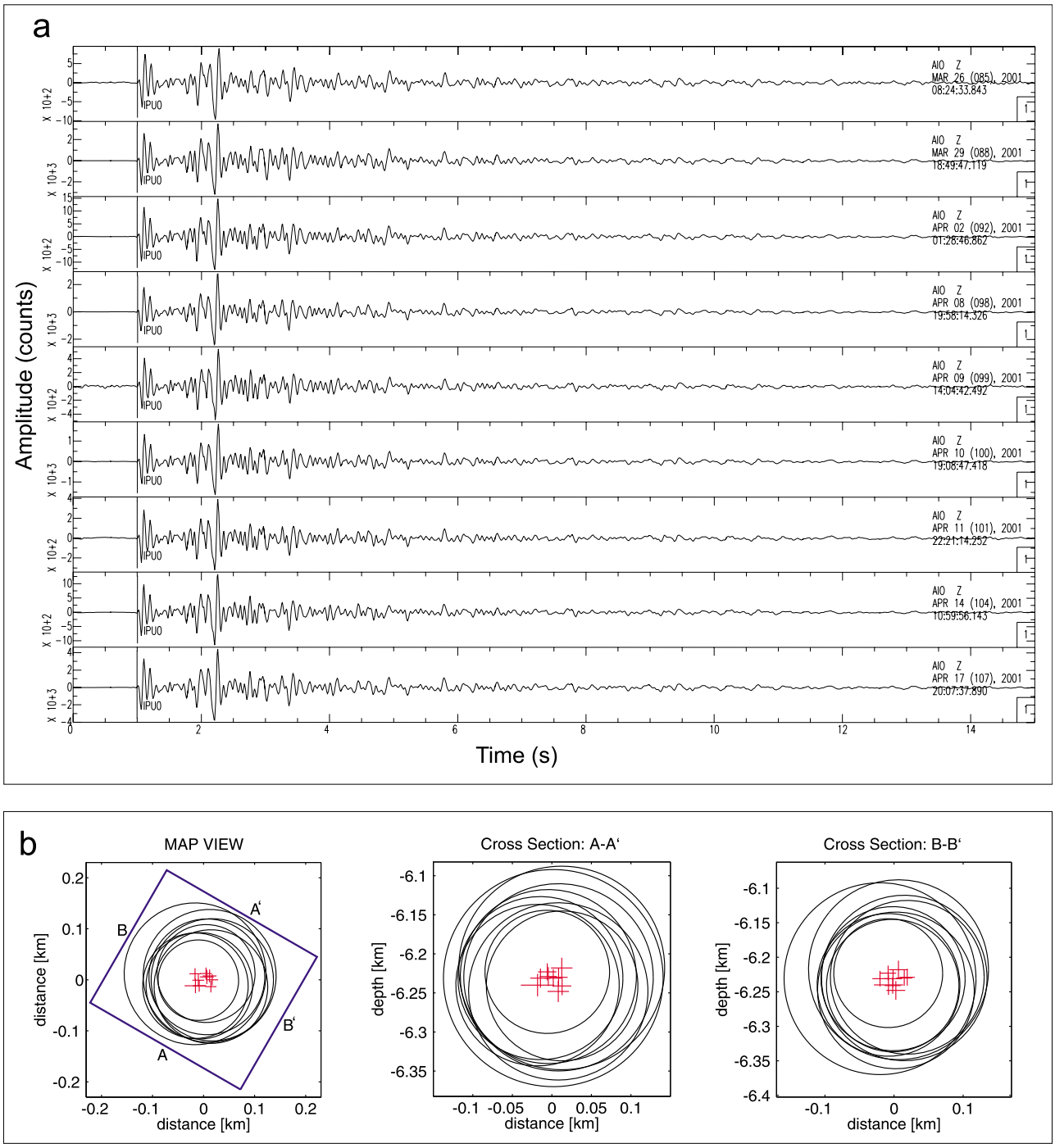

Figure 3. (a) Waveforms for the multiplet 4 (M4). Example of repeating earthquakes recorded by station AIO, extracted from the 2001 swarm, using a cross-correlation threshold of 0.9. Note the high similarity of the waveforms through the entire coda. (b) Map view and cross sections of the relative hypocenter locations for M4, obtained with relative relocation using a double difference algorithm (HypoDD), the average uncertainty is less than 20 m in both vertical and horizontal directions, indicated by the size of the crosses. Approximate rupture patch dimensions are also plotted as circles.

difference technique [*Waldhauser and Ellsworth*, 2000]. By cross-correlating windows containing *P* and *S* wave arrivals, we obtained differential traveltime measurements for all possible combinations of event pairs within an individual multiplet. From these, we use the HypoDD algorithm to minimize errors due to the velocity model and compute the interevent distances of events within each multiplet, with a reduced location error of an order of magnitude compared with the catalog locations. Figure 3b shows the relative hypocentral distance between events of a multiplet extracted from the 2001 swarm. The event hypocenters are located within an area of ~50 m^2 with an average uncertainty in

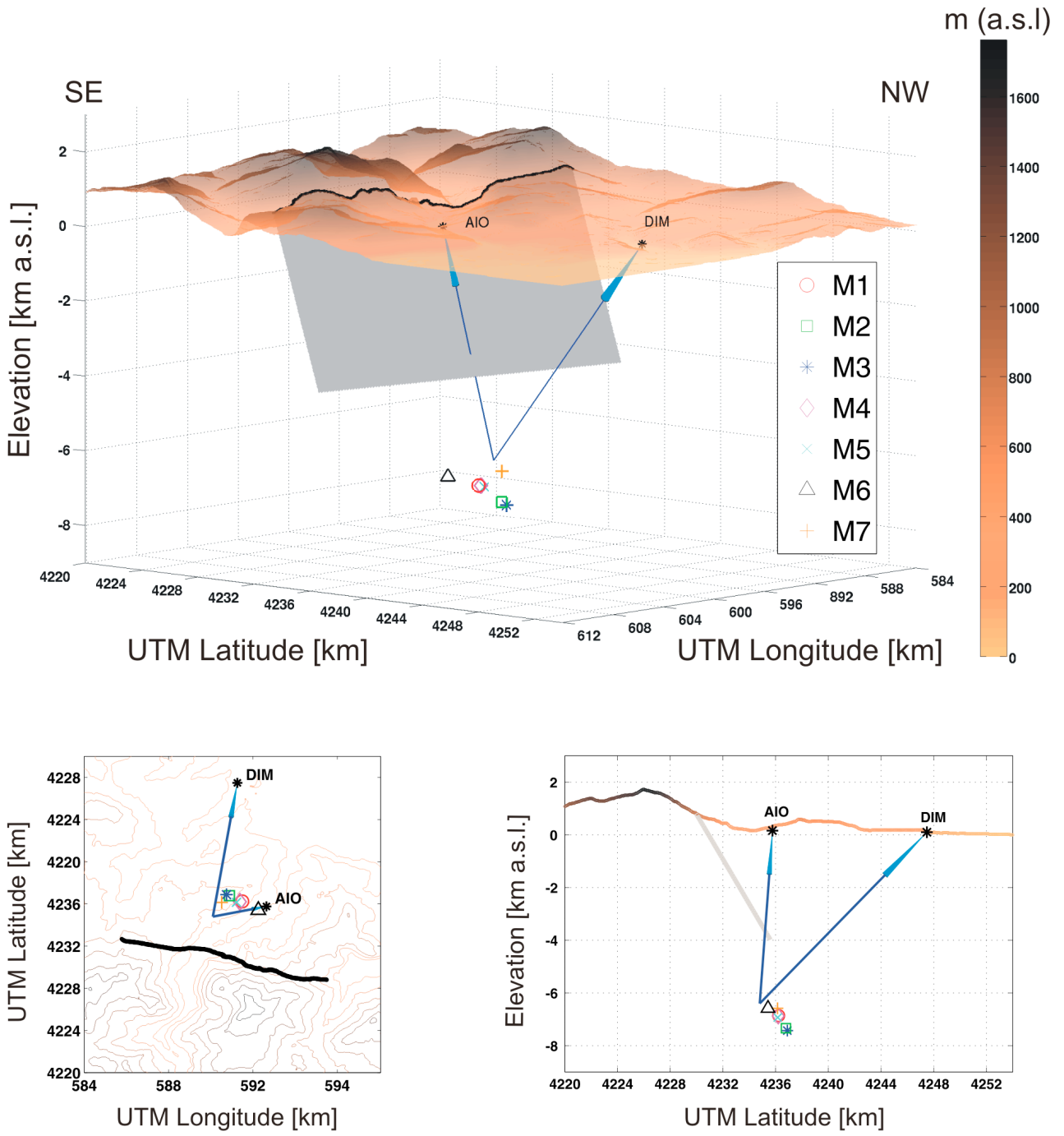

Figure 4. (top) 3-D map of the southern shore of the Gulf of Corinth. The different symbols correspond to the families of repeating earthquake extracted from the 2001 swarm after relocation. The rectangular plane represents the Pyrgaki fault zone with respect to AIO and DIM stations. The two arrows indicate the vectors between the Agios Ioanis earthquake and AIO and DIM stations, 7.1 and 9.2 km, respectively. (bottom left) Map view and (bottom right) S-N cross section.

relative location of less than 20 m in both horizontal and vertical directions. In addition, we estimated the earthquake source dimension using the scaling relation for a circular crack [*Kanamori and Anderson*, 1975] to limit our analysis to families of event that are very close in space (Figure 3b). All events rupture approximately the same fault patch, with patch lengths ranging between 150 and 300 m for multiplet events with magnitude ranging between 1.5 and 2.5.

[13] Although the events within a multiplet are relocated relative to each other with high precision, the absolute location of the multiplet itself still maintains the original location error. The absolute positions of each multiplet shown in Figure 4 were computed by *Pacchiani* [2006]

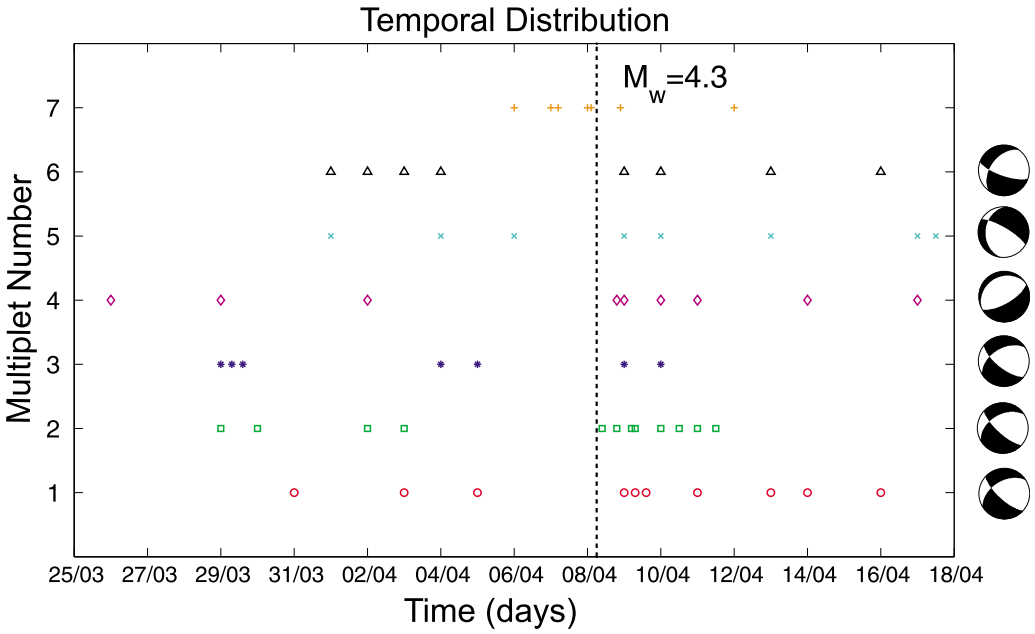

Figure 5. Temporal distribution of all events belonging to the seven multiplets analyzed. The dashed line marks the occurrence of the 2001 $M_w = 4.3$ event (8 April 2001 at 0612). The different symbols correspond to different multiplets. (right) Representative focal mechanisms for families M1–M6, showing the associated planes (data after *Pacchiani et al.* [2006]).

inverting with HypoDD, set to singular value decomposition mode, the delays of the absolute wave arrival times for all pairs or reference earthquakes. The absolute position of the multiplets show minimal spatial variability, in particular, the average distance between the centroid of each family of repeating earthquakes, and the Agios Ioanis event is around 1550 m for five multiplets (M1, M2, M3, M4, and M5) and around 2183 and 813m for M6 and M7, respectively (Figure 4). The temporal distribution of the events within each of the seven multiplets used in the CWI analysis is shown in Figure 5.

3. Method: Coda Wave Interferometry

[14] The late part (coda) of a seismic signal is composed of multiply scattered waves that repeatedly sample over an expanding region around the source. The coda wave interferometry (CWI) method exploits this multiple-sampling characteristic to infer small changes in the velocity of the medium. The CWI theory is based on path summation; the total wavefield is expressed as the superposition of the waves that propagate along all scattering paths [*Snieder*, 2006; *Snieder et al.*, 2002]. A homogeneous change in the seismic velocity of propagation affects the time lag (τ) between two seismic traces recorded before and after the perturbation occurred. The longer the waves travel within the medium, the more they are affected by the velocity variations. The changes in the waveforms $u(t')$ and $\tilde{u}(t')$ can be quantified by computing the time-shifted cross correlation,

$$R(\tau) = \frac{\int_{t-T}^{t+T} u(t')\tilde{u}(t'+\tau)\mathrm{d}t'}{\left(\int_{t-T}^{t+T} u^2(t')\mathrm{d}t' \int_{t-T}^{t+T} \tilde{u}^2(t')\mathrm{d}t'\right)^{1/2}}, \quad (1)$$

for windows centered at time t with a window length of $2T$. The CWI technique involves comparing small parts of the two aligned signals by calculating the time lag (τ) corresponding to the maximum of the cross correlation for sliding windows. The relative velocity change for each time window is given by the formula,

$$\frac{\mathrm{d}v}{v} = -\frac{\tau}{t}. \quad (2)$$

In the case of a homogeneous velocity change, the lag time varies linearly with time and the mean velocity variation is proportional to the slope $\frac{\mathrm{d}v}{v}$. For each pair of repeating events, we aligned the two seismograms at the P arrival and visually inspected the waveforms to asses the similarity of the first arrivals. Using nonoverlapping moving windows of eight cycle lengths with respect to the central frequency (~8 Hz), the time lag (τ) was computed along the length of the waveforms. The percentage of velocity variation between two waveforms was retrieved by fitting the slope with a linear regression curve through a least squares solution. The operation was performed through the correlated waveforms until the variance of the travel time perturbation for waves arriving within the time window [*Snieder et al.*, 2002] becomes unstable. The error of the line fit (regression error) is estimated by computing the root mean square over the residuals. The CWI technique was applied to all possible combinations of doublets within each multiplet recorded by stations AIO and DIM, thus obtaining over 340 values of velocity change.

4. CWI Results

4.1. Preseismic and Postseismic Velocity Changes

[15] To investigate the preseismic and postseismic effect of the $M_w = 4.3$ earthquake on the surrounding medium, we

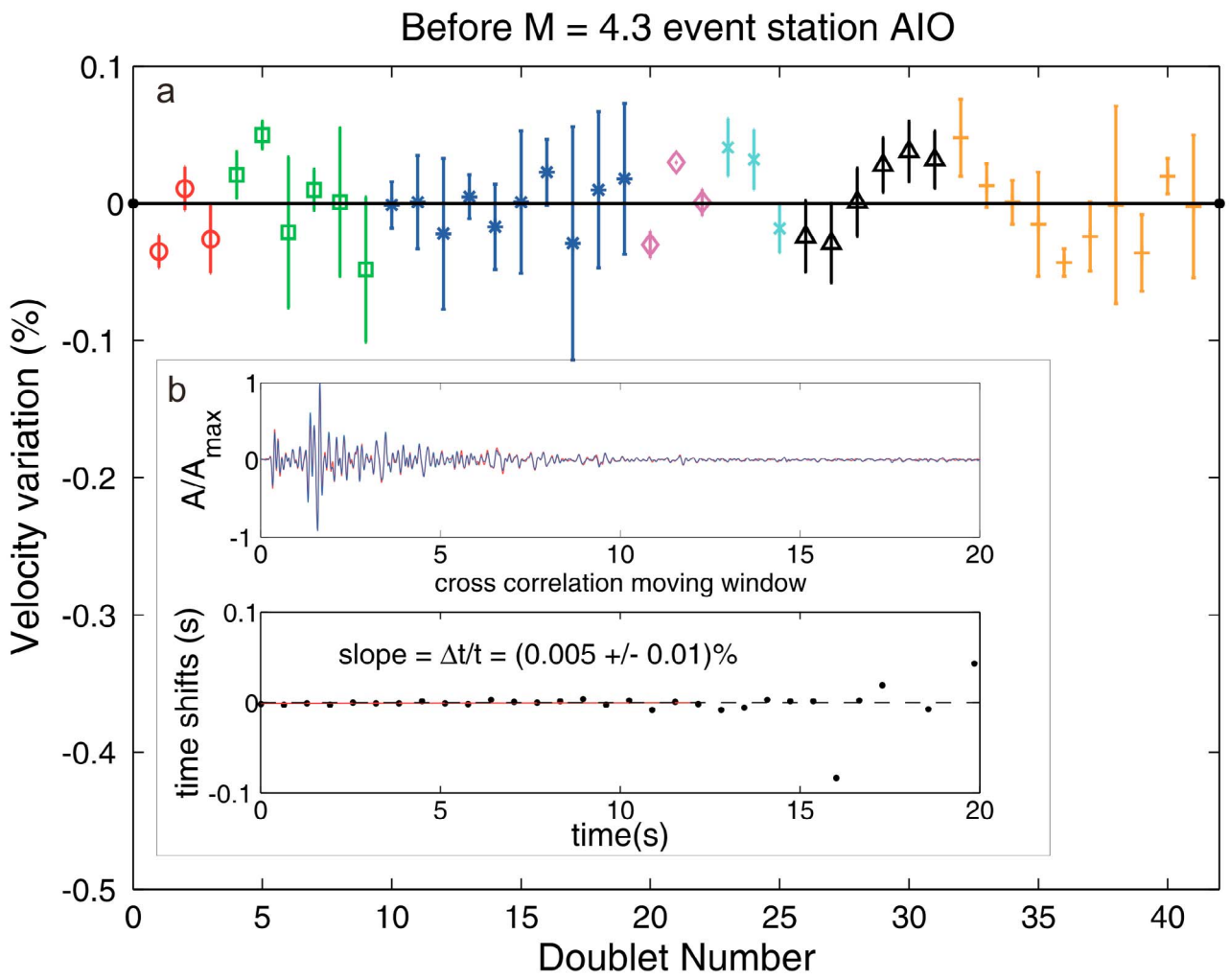

Figure 6. (a) The results of CWI analysis applied to all the doublets recorded before the $M_w = 4.3$ event for the seven families of repeating earthquakes. Symbols correspond to those used in Figure 5 for each family. There is no trend in the velocity variation, values are around 0 ± 0.05%. (b) (top) Doublet belonging to M3, the two waveforms are extremely similar and show high coherency. (bottom) Result from an application of the CWI to the same doublet: the dots represent the time lag corresponding to the maximum cross correlation for each time window. The thin solid line shows the calculated slope. The events indicate no velocity change.

analyzed the velocity variations between all possible combinations of repeating earthquake pairs recorded by station AIO, before and after its occurrence, for all seven multiplets. Figure 6a shows the percentage variation in the seismic velocities between two event pairs for each family, where both events in the family occur before the Agios Ioanis earthquake. Figure 6b shows the application of CWI to a doublet of M3. The two earthquake waveforms are very similar, even in the late coda. The similarity in the direct arrivals suggests that the two earthquakes have virtually identical source location and focal mechanism. The absence of any significant time shift between the late coda of the two waveforms qualitatively indicates that the elastic properties of the medium remained unchanged during the inter-event time interval. This is quantitatively confirmed by the stability around zero of the measured time lag (τ), for all the windows along the coherent signal. The slope is zero within measurement error. None of the doublets in Figure 6a show any significant change in the mean velocity of propagation. This suggests that no significant preseismic change occurred in the medium sampled by the coda waves and precludes the presence of any quantifiable precursor signal.

[16] While the multiplets M3 and M7 only cover a temporal window of 4 days after the $M_w = 4.3$ event (Figure 5), M1, M4, M5, and M6 enable us to monitor the postseismic velocity of the medium up to 9 days following the Agios Ioanis earthquake (Figure 7). The application of CWI to a doublet within M6 is shown in Figure 7b. As in the case of doublet pairs occurring before the $M_w = 4.3$ event, doublets in which all event pairs occur after the Agios Ioanis event show no significant velocity changes. Thus, for at least 9 days after the $M_w = 4.3$ event, no measurable postseismic changes in the sampled medium occurred. Unfortunately, AIO station failed 10 days after the Agios Ioanis event.

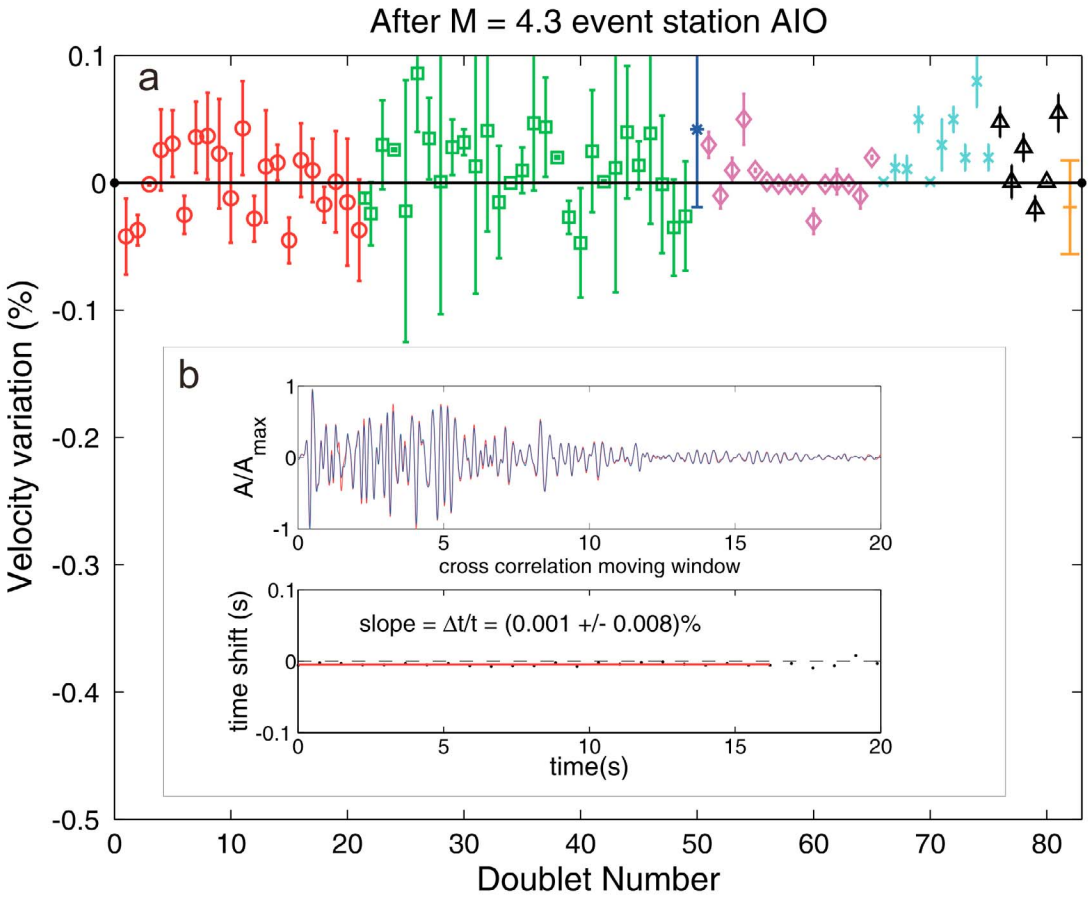

Figure 7. (a) Velocity variation, computed with CWI on doublets post-Agios Ioanis event. No significant trend in velocity variation was found. Combining M1, M2, M4, M5, and M6 gives the good temporal sampling in the 9 days following the Agios Ioanis event. (b) (top) Event pair post-Agios Ioanis event showing an exceptional high coherency up to 20 s. (bottom) CWI on the doublet pair, the time lag (dots) is stable around zero.

4.2. Coseismic Velocity Changes

[17] To complete the assessment of temporal variations of the medium velocities, we analyzed all doublets where one event in the pair occurs before and one occurs after the M_w = 4.3 event. The corresponding CWI results, summarized in Figure 8a, show that five multiplets (M1, M2, M3, M6, and M7) were clearly affected by a consistent decrease in the seismic velocity. The mean velocity decrease for these multiplets ranges between −0.1% and −0.3% (Figure 8a). Analysis of two multiplets, M4 and M5, yields an order of magnitude smaller velocity changes (−0.02%) than the one experienced by the other multiplets; we consider them to be at the limit of significance yet still exhibiting a general negative trend. Figures 8b and 8c show a comparison between two doublets, belonging to M5 and M2, considered representative of a insignificant and significant velocity change, respectively. While events in M5 (Figure 8b) show no temporal "stretching" in the coda, implying no changes in the mechanical properties, there is an unambiguous time shift in the waveforms for the events in Figure 8c, corresponding to a change in wave speed estimated to be −0.19% ± 0.03%. The different coseismic velocity variations sampled by the seven multiplets imply that the causative perturbation is spatially variable.

[18] To temporally constrain the period in which changes in the velocity of the medium occurred, and therefore constrain the interpretation of the mechanism causing the change, we exploit M7. This multiplet was chosen because it has a good temporal resolution around the occurrence time of the Agios Ioanis earthquake (Figure 5). The inset in Figure 8 shows the velocity variation between each individual earthquake in the M7 multiplet family and the first event of the multiplet. The earthquakes that nucleated up to 1 h prior the Agios Ioanis event experienced a velocity change with respect to the first event in the family, which is approximately zero. Hence no preseismic change is evident. However, the first postseismic event, which occurred 18 h after the Agios Ioanis event, shows a 0.2% decrease in the seismic velocity. Applying the same analysis to the M2 multiplet constrains the velocity reduction to have occurred within 5 h after the M_w = 4.3 event.

[19] Therefore, we conclude that the temporal window in which the velocity perturbation occurred is from 1 h before to 5 h after the main shock. This suggests that the Agios

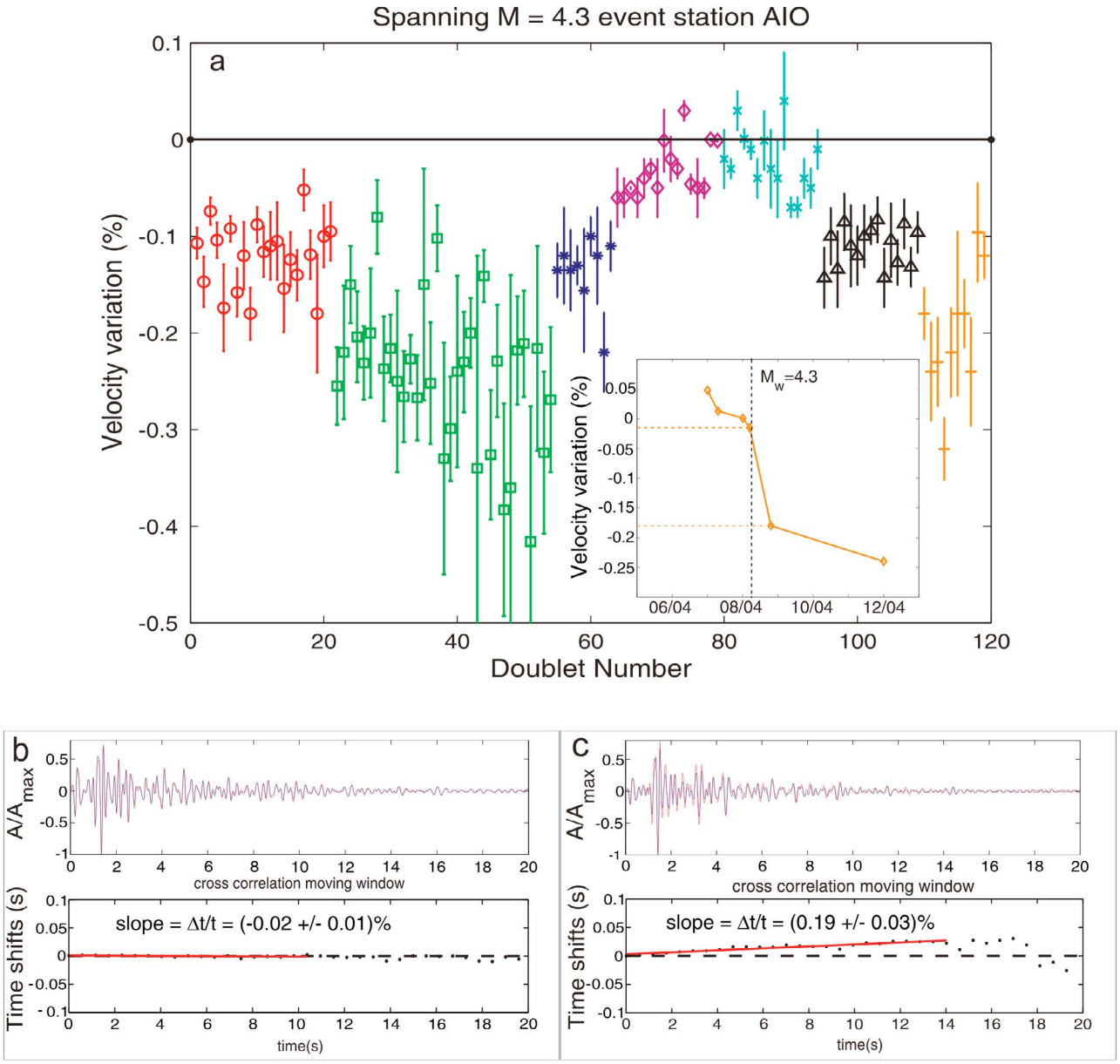

Figure 8. (a) Variations in the seismic velocity between paired sets of repeating earthquakes where one event in the doublet nucleates before and one after the Agios Ioanis event. The average velocity variations detected by five of the seven multiplet families (M1, M2, M3, M6, and M7) ranges between −0.1% and −0.3%. The average velocity variation detected by two families (M4 and M5) is around −0.02%. Inset, the temporal evolution of multiplet 7 (M7) relative to the first event in the multiplet shows a clear coseismic signal. (b) A pair of repeating earthquakes belonging to M5 superimposed and aligned at the *P* arrival and waveform cross correlation of pairs. (c) A pair of repeating earthquakes belonging to M2 and waveform cross correlation, the lag time (dots) linearly increase with time. A decrease in the seismic velocity of about 0.2% is estimated based on the slope.

Ioanis earthquake is highly likely to be the source of the perturbation in the medium properties, causing the coseismic decrease in the seismic velocity of propagation exhibited in the Keritinis multiplets. All the earthquakes belonging to the seven multiplets, previously analyzed with CWI at station AIO, were also recorded at DIM station, and most of them, with good signal-to-noise ratio, were analyzed for velocity changes at DIM. Figure 9 shows the velocity changes for events spanning the time of the Agios Ioanis earthquake recorded at the station DIM. None of the multiplets recorded by station DIM exhibit a coseismic decrease in the seismic velocity (Figure 9).

4.3. Outliers

[20] Two of the studied multiplets recorded at AIO, M4 and M5, were found to be insensitive to the coseismic perturbation associated with the Agios Ioanis event, even though the relative position of the seven families is only a

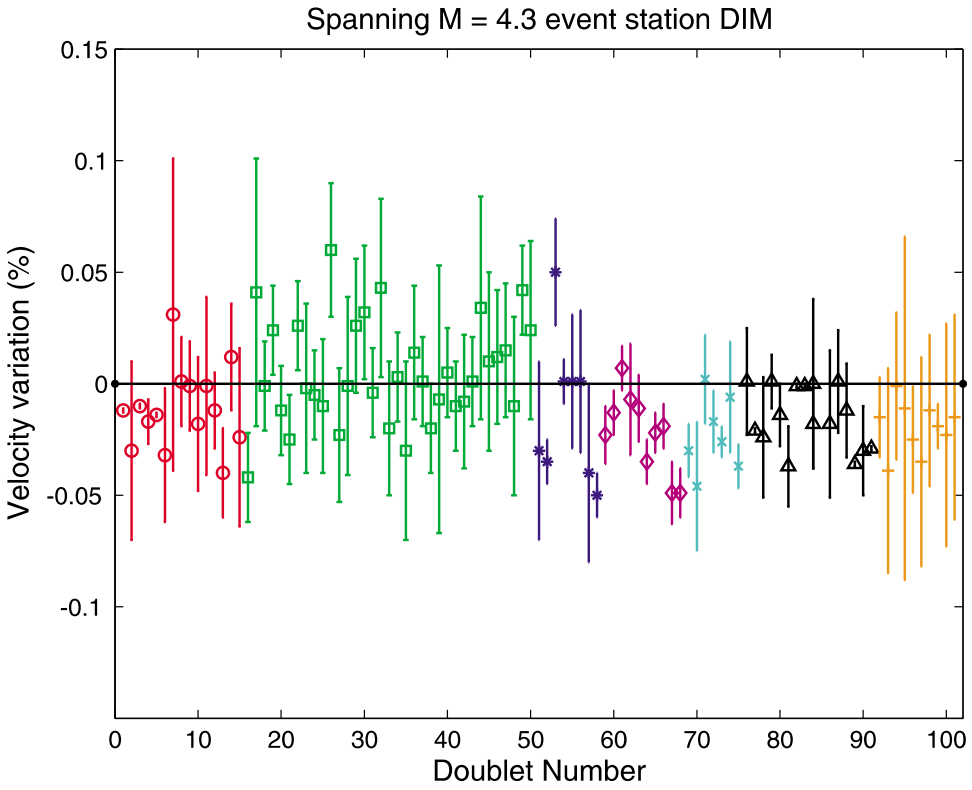

Figure 9. Velocity analysis carried out on doublets, M1, M2, M3, M6, M7, spanning the time of the Agios Ioanis earthquake, recorded by station DIM. There is no a significant change in the velocity of the medium for events recorded at DIM.

few hundred meters apart (Figure 4). A different radiation pattern and hence different volume sampled by the coda waves, compared to the other families, might be a possible reason for this observation. All the events of each multiplet have virtually colocated sources and similar rupture mechanisms, therefore only one event is necessary to describe the focal mechanism of the whole family. The representative focal mechanism for six families (M1–M6) [*Pacchiani*, 2006] is shown in Figure 5. Multiplets M1, M2, M3, and M6, which were found to be sensitive to the coseismic change, have very similar focal mechanisms while the two multiplets, M4 and M5, unaffected by the velocity perturbation, show different focal mechanisms.

5. Constraining the Physical Mechanism

[21] To understand which mechanism possibly caused the measured coseismic velocity variations induced by the Agios Ioanis earthquake, we tested several hypotheses. The decrease in the seismic velocity of propagation may have been caused by (1) an increase in the crack density in the near surface because of strong ground motion (dynamic effect), (2) a decrease in the fracture stiffness caused by a reduction of the normal stress applied to the fault zones in the neighborhood of the Agios Ioanis event (static effect), and (3) a variation of the pore pressure in neighboring fault zones, which may have been generated by both static and dynamic stress changes.

5.1. Dynamic Stress Changes

[22] Recent studies have successfully detected perturbations generated by seismic transient oscillations and show common and persistent characteristics. These consist of (1) a systematic behavior of the temporal changes affecting different stations, (2) increase of time delays with increasing peak ground acceleration [e.g., *Peng and Ben-Zion*, 2006], (3) greater changes observed at soft rock sites, and (4) a very fast (days) post-main shock recovery of the damaged shallow rock [e.g., *Rubinstein and Beroza*, 2004; *Vidale and Li*, 2003]. In order to determine whether the dynamic effect is the cause of the observed changes in the seismic velocities, we analyzed the main characteristics described above, which are usually associated with this mechanism.

[23] Using the information extracted from the seismic waves of multiplets, we compare the dynamic effect of the $M_w = 4.3$ Agios Ioanis earthquake at stations AIO and DIM. They are located 7.1 and 9.2 km from the Agios Ioanis earthquake, respectively (Figure 4), and they are subjected to the same order of magnitude of peak ground acceleration (PGA) up to 0.1 g (Figure 2). While station AIO is installed directly in limestone bedrock, station DIM is buried in a softer subsurface characterized by Pliocene delta conglomerate. We cannot test hypothesis (1) and (2) as we only use two stations, AIO and DIM, and the subsurface geology of these two sites are different and therefore not comparable.

[24] According to hypothesis (3), a change in the shallow crust caused by dynamic shaking should have predominantly affected the multiplets recorded at station DIM as it is

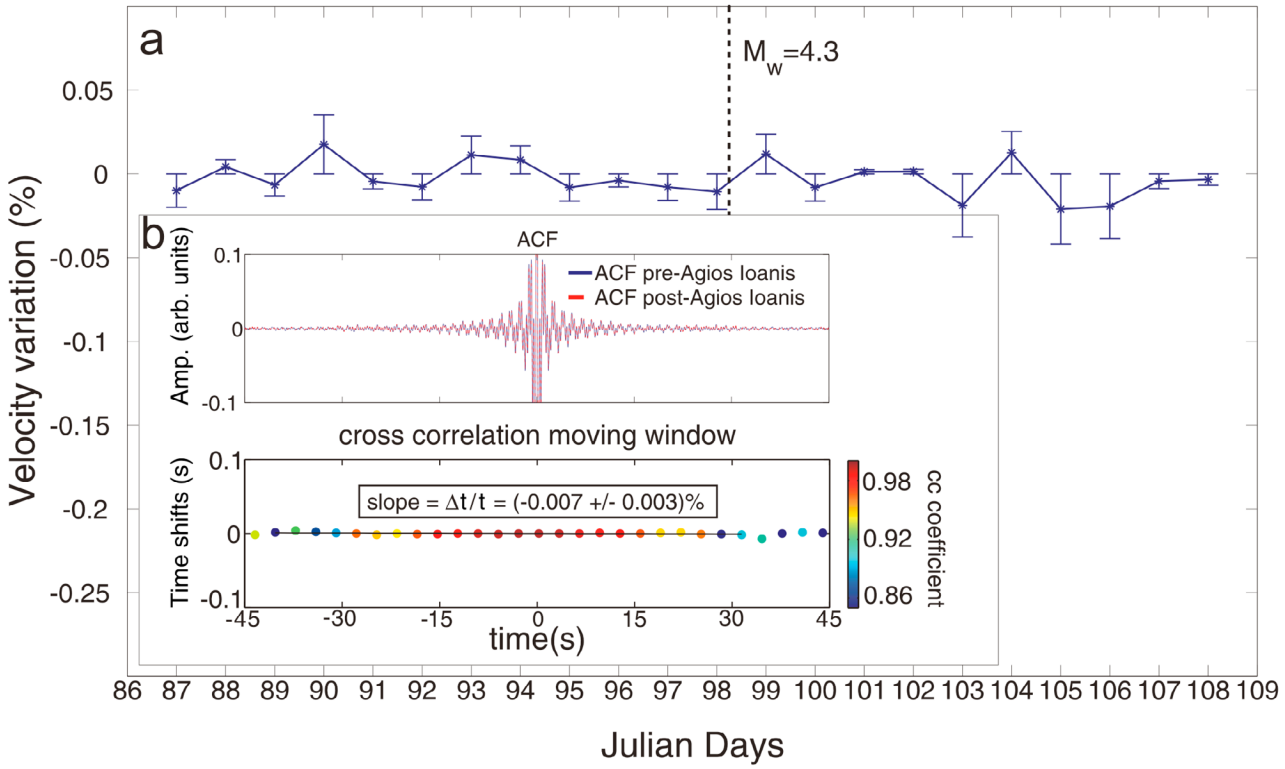

Figure 10. (a) Relative velocity changes calculated from AIO data with the PII technique. The error bar corresponds to the uncertainty of the linear slope estimation. (b) (top) Averaged autocorrelation function (ACF) before (blue) the $M_w = 4.3$ event (87–97 Julian days) superimposed to the averaged ACF after (red) the Agios Ioanis earthquake (98–108 Julian days). (bottom) Time shift-averaged measurement between the pre-"main shock" ACF and post-"main shock" ACF. The color of the dots (time lag) indicate the maximum cross-correlation values for each time window.

installed in softer material. However, while we do detect velocity changes between doublets recorded at station AIO (Figure 8a), we do not detect any significant coseismic velocities changes recorded at station DIM (Figure 9). These results do not support hypothesis (3) and indicate that the volume of crust between the source region and station DIM is not affected by any significant coseismic change in elastic properties. However the same multiplets were sensitive to a decrease in the seismic velocities.

[25] There is, however, a more robust way of assessing the dynamic shaking hypothesis. If we assume that the dynamic shaking is the main cause of a change in the crack density in the near surface around, this should have similarly affected all the multiplets recorded at the station. This assumption however is not supported by our observations; in fact, event pairs belonging to two multiplets (M4 and M5) recorded at station AIO do not detect any significant change, as shown in Figure 8a.

[26] We also tested whether our data support the hypothesis of a postseismic healing of the crust, which is often an observed consequence of strong ground motion-induced near-surface damage [e.g., *Li et al.*, 2006; *Peng and Ben-Zion*, 2006; *Vidale and Li*, 2003]. In studies with good postseismic temporal sampling, changes in the medium velocity caused by moderate to large earthquakes have been seen to start recovering after only a few days [e.g., *Li et al.*, 2006; *Peng and Ben-Zion*, 2006]. In some cases, the healing process lasts up to years revealing a logarithmic time signature [e.g., *Schaff and Beroza*, 2004; *Vidale and Li*, 2003] which has been interpreted as the closure of near-surface crack opened during the main shock [e.g., *Li et al.*, 2006; *Peng and Ben-Zion*, 2006]. In our case, however, we do not detect any postseismic variations in the seismic velocity of propagation in the first 9 days after the main shock (Figure 7a), indicating that the rapid or logarithmic healing process observed in other localities did not occur.

[27] To further investigate the possibility of a change in the shallow crust and thus better constrain the causative mechanism for the measured seismic velocity variations, we utilized the passive image interferometry (PII) technique [*Sens-Schönfelder and Wegler*, 2006; *Wegler et al.*, 2009; *Wegler and Sens-Schönfelder*, 2007]. This method is based on the idea that the average cross-correlation function (CCF) between random fields, such as ambient seismic noise and scattered coda waves, recorded at two stations, differ from the Green's function between these two points solely by an amplitude factor [e.g., *Paul et al.*, 2005; *Sabra et al.*, 2005]. We extracted daily source-receiver colocated Green's functions from the averaged autocorrelation function (ACF) of seismic noise recorded at station AIO. The ACF is representative of the state of the medium, near the station, and can be thought of as a zero offset Green's function. We searched for temporal changes of the elastic properties of the shallow crust by comparing (using CWI

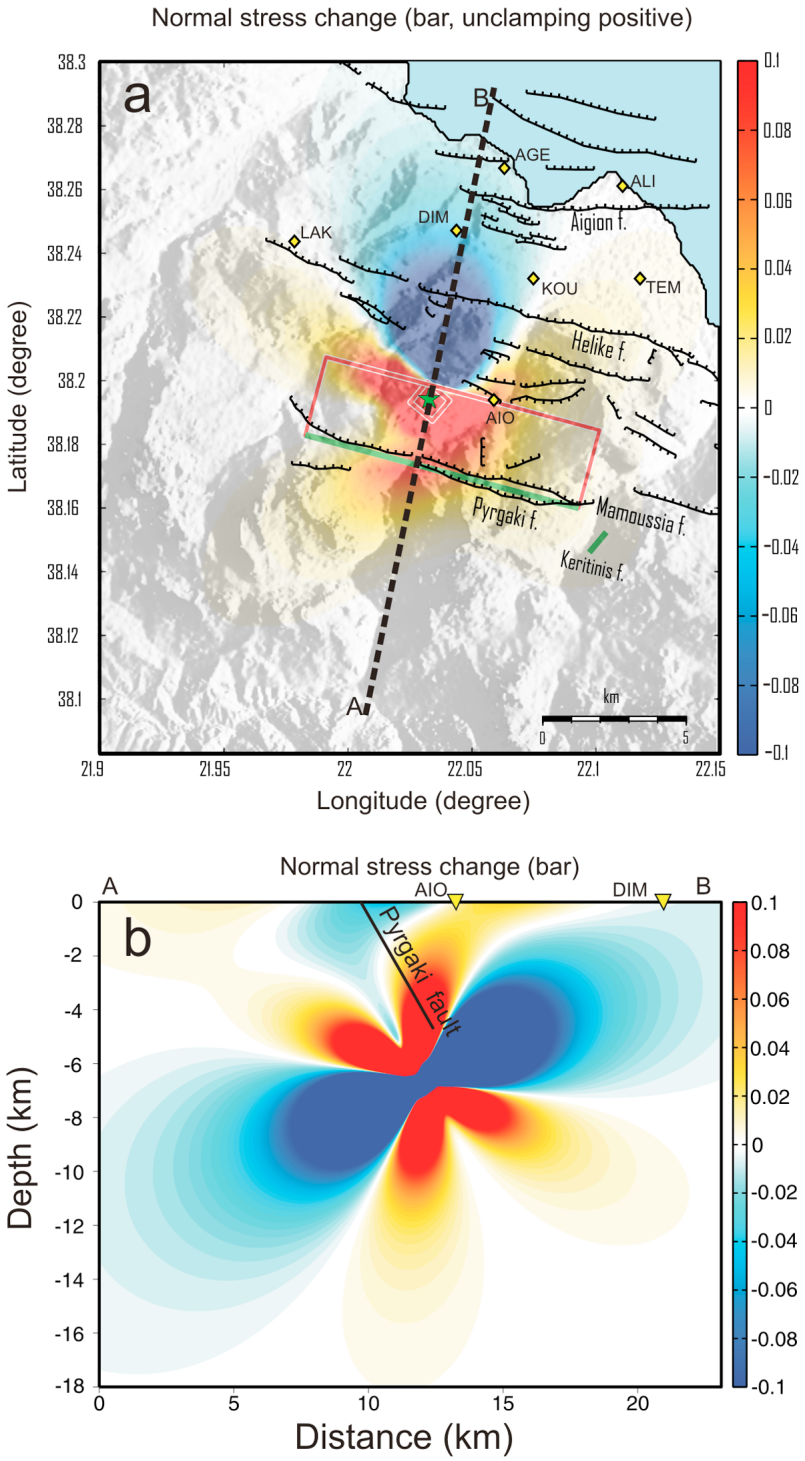

Figure 11. Static stress changes induced by the M_w = 4.3 earthquake calculated on planes parallel to Pyrgaki fault. (a) Mean values of normal stress changes computed between 3 and 5 km and projected on the surface, the red color corresponds to the unclamping of the faults parallel to Pyrgaki. The star represents the epicenter of the Agios Ioanis earthquake, and the two green lines correspond to the intersection with the surface of the two modeled faults, Pyrgaki and Keritinis. (b) Vertical cross section along the dashed line showing values of normal stress changes.

analysis) a reference ACF function, defined as the average ACF function for the whole period (22 days), with each daily computed ACF function. Figure 10a shows the evolution of the obtained relative velocity change measured at AIO station. No coseismic change is observed, indicating that the coseismic perturbation observed with the CWI analyzes of the multiplets (Figure 8a) is not likely to occur in the shallow crust. In Figure 10b (inset), we show the

superimposed averaged ACF generated for noise data before and after Agios Ioanis earthquake. The two signals are very similar, and the waveform cross correlation shows a near-zero slope, indicating the absence of a coseismic change in the seismic velocity of the shallow crust.

5.2. Static Stress Changes

[28] In the previous section, we argued that the near-surface effect caused by the dynamic shaking associated with the Agios Ioanis earthquake is not the main cause of the measured velocity changes. Our objective in this section is to determine whether the observed coseismic decrease in the seismic velocities might have been caused by a change in the static stress field generated by the coseismic deformation following the M_w = 4.3 earthquake. Therefore, we modeled the normal stress changes induced by the Agios Ioanis earthquake on planes that are oriented parallel to the Pirgaki fault (Figure 11a), using the Coulomb 3.1 software [*Lin and Stein*, 2004; *Toda et al.*, 2005]. The orientation of the source fault is taken from *Zahradnik et al.* [2004]. The model predicts that faults and fractures that are parallel to the dominant fault trend on the southern shore of the Gulf (e.g., Pirgaki fault) and located in the volume of crust between the main shock rupture and station AIO, are expected to be unclamped as a consequence of a reduction in normal stress (Figure 11b). Unclamping the neighboring fault system would increase its compliance reducing seismic waves velocities. According to the modeled stress changes, the fractured volume of medium between the Agios Ioanis event and station DIM is subjected to an increase in the applied normal stress (Figure 11b), and therefore, it is expected to be stiffer. As a consequence, one would expect to measure a positive change in the seismic velocities between postseismic and preseismic events recorded at DIM, in contrast with our results (Figure 9), which show no change. However, the stiffness is not a linear function of the normal stress [*Pyrak-Nolte and Morris*, 2000; *Pyrak-Nolte et al.*, 1990] and, therefore for the same absolute stress change, it is more difficult to stiffen a fractured rock than it is to increase its compliance. Importantly Figure 11a highlights that stations AIO and DIM are located in areas of decreased and increased normal stress, respectively. However in the cross sections (Figure 11b), it is clear that stress changes in the shallow crust underneath AIO and DIM stations are either very small or negligible. This is an indication that the observed velocity variations are not caused by a static near surface change in the elastic properties of the medium but more likely in the seismogenic zone. Data from Figure 10 also favor a deeper origin.

[29] The question arises as to whether the small coseismic changes in the static stress could have caused the observed 0.1%–0.3% decrease in the seismic velocity. Stress changes in compliant material can, in theory, be estimated at depth by combining very precise fractional velocity measurements ($dv/v = \delta v$) and a sensitivity factor of the velocity (η) [*Silver et al.*, 2007]. *Niu et al.* [2008] measured the stress sensitivity factor in the SAFOD drill site, California, at a depth of 1 km, using known atmospheric stress loading. Applying the relation $\delta\sigma = \delta v/\eta$, where $\delta\sigma$ is the stress perturbation, they determined stress changes caused by two earthquakes from fractional observed velocity variations. Here we used the same approach to estimate the amount of stress change needed to cause the measured velocity reduction and thus check if the modeled static stress changes are in agreement with the measured velocity variations. Although the stress sensitivity factor will likely be site dependent, we used the value obtained by Niu et al., as it is the only available estimate at depth (1 km). Using the stress sensitivity measured by Niu et al. (2.4×10^{-7} Pa^{-1}) and the precise measurements of fractional velocity changes determined in the Gulf of Corinth using CWI (0.001–0.003), we predicted stress changes that range from 0.04 to 0.12 bars. These values correspond to the stress changes modeled for a depth range of 3–5 km on faults with orientations parallel to Pyrgaki fault. This indicates very good agreement between stress changes predicted by the static stress model and inferred stress changes from the observed velocity variations.

5.3. Static Stress Effect

[30] In the previous sections, we showed that the measured velocity changes in the medium elastic properties are likely unassociated with damage of the shallow crust caused by the transient oscillations generated by the M_w = 4.3 earthquake. The source of the observed velocity reductions are therefore probably located deeper within the volume of the medium between the repeating earthquakes and station AIO. Preferred hypotheses for the velocity changes are therefore (1) a change in the pore pressure or (2) an increase in the fracture compliance.

[31] The possibility of a coseismic perturbation in the velocity caused by changes in the pore pressure in the Pyrgaki fault zone is considered. *Pacchiani and Lyon-Caen* [2009] strongly suggested the involvement of fluids in the 2001 earthquake swarm by showing that the observed earthquake migration is explained by pore pressure diffusion [*Pacchiani and Lyon-Caen*, 2009]. However, a coseismic alteration in the pore pressure caused by a transient stress change should be accompanied by a rapid postseismic change in the medium properties. We have shown in Figure 7a the absence of a postseismic signal affecting the multiplets, and therefore, we infer that the mechanism for the coseismic change is probably not attributable to a fluid pressure variation in the Pyrgaki fault zone caused by dynamic shaking. However, since we do not have data after 18 April 2001, any variation occurring beyond this date is unknown and we cannot conclusively rule out changes in fluid pressure caused by static stress changes as the mechanism for the observed velocity variations.

[32] However, the very good agreement between the stress changes predicted from the seismic data and those predicted by modeling stress redistribution following the Agios Ioanis event favor the role of solid-mechanical compliance changes.

6. Conclusions

[33] The occurrence of families of very similar earthquakes on the southern shore of the Gulf of Corinth, Greece, enabled us to study in detail the temporal evolution of the seismic wave velocities in the rock volume neighboring the M_w = 4.3 Agios Ioanis earthquake. Using the coda wave interferometry (CWI) method, we obtained information about high-precision velocity changes, enabling us to

measure a very clear coseismic reduction of the path-averaged seismic velocity in the medium of about 0.2% following the Agios Ioanis event. The temporal resolution of the repeating events constrains the perturbation to have occurred within 1 h before and 5 h after the Agios Ioanis earthquake, indicating that the M_w = 4.3 earthquake is highly likely the cause of the changes. The absence of preseismic and postseismic variations indicates that the changes are neither due to an accumulated effect of many small events nor caused by a change in fluid pressure in the Pyrgaki the fault zone, which sits above the Agios Ioanis hypocenter.

[34] Careful analyzes of the nature of the changes, combined with a temporal study of the source-receiver colocated Green's functions, revealed that the perturbation causing the velocity variations is spatially localized at depth. Moreover, the observed changes do not show characteristics compatible with a transient stress change. Therefore, dynamic shaking, a very commonly observed source of coseismic changes in the crust, is probably not the cause of the reduction in seismic velocity. Instead, a change in the normal stress applied to the Pyrgaki fault zone explains the coseismic decrease in seismic velocity very well. The magnitude, spatial distribution, and temporal evolution of velocity variations observed support the hypothesis that the static stress change induced by the Agios Ioanis earthquake is the causative mechanism. As large faults are more compliant than small faults [*Worthington and Lubbe*, 2007] and thus more sensitive to changes in the applied stress, we expect that the measured velocity changes are biased toward the biggest fault closest to the seismogenic depth. Therefore, we suggest that a deep part of Pyrgaki fault zone (3–5 km) was unclamped by a static stress change induced by the Agios Ioanis earthquake. These observations complement dynamic and static stress modeling as a means of tracking the temporal evolution of stress on fault systems. They also have specific implications for seismic hazard in the Gulf of Corinth.

[35] **Acknowledgments.** This research was funded by Science Foundation Ireland (SFI, grant 06/RFP GEO 005). This work was partially supported by the European Commission project 3HAZ-Corinth. We would like to thank Martin Möllhoff for technical support and Pascal Bernard and our colleagues from Seismology and Computational Rock Physics Laboratory for interesting discussions. Thanks to two anonymous reviewers and to the Associate Editor for helpful comments. Use of generic mapping tools (GMT) (http://gmt.soest.hawaii.edu) and Coulomb 3.1 software (http://quake.wr.usgs.gov/research/deformation/modeling/coulomb/) is acknowledged.

References

Bokelmann, G. H. R., and H. P. Harjes (2000), Evidence for temporal variation of seismic velocity within the upper continental crust, *J. Geophys. Res.*, *105*, 23,879–23,894.

Geller, R. J., and C. S. Mueller (1980), Four similar earthquakes in Central California, *Geophys. Res. Lett.*, *7*, 821–824.

Giurgea, V., D. Rettenmaier, L. Pizzino, I. Unkel, H. Hötzl, A. Förster, and F. Quattrocchi (2004), Preliminary hydrogeological interpretation of the Aigion area from the AIG10 borehole data, *C. R. Geosci.*, *336*, 467–475.

Gret, A., R. Snieder, and U. Ozbay (2006), Monitoring in situ stress changes in a mining environment with coda wave interferometry, *Geophys. J. Int.*, *167*, 504–508, doi:510.1111/j.1365-1246X.2006.03097.x.

Hill, D. P., et al. (1993), Seismicity remotely triggered by the magnitude 7.3 Landers, California, earthquake, *Science*, *260*, 1617–1623.

Johnson, P. A., and X. Jia (2005), Nonlinear dynamics, granular media and dynamic earthquake triggering, *Nature*, *437*, 871–874, doi:810.1038/nature04015.

Kanamori, H., and D. L. Anderson (1975), Theoretical Basis of Some Empirical Relations in Seismology, pp. 1073–1095.

King, G. C. P., R. S. Stein, and J. Lin (1994), Static stress changes and the triggering of earthquakes, *Bull. Seismol. Soc. Am.*, *84*, 935–953.

Lee, W. H. K., and J. C. Lahr (1972), A computer program for determining hypocenter, magnitude, and first motion pattern of local earthquakes, *U. S. Geol. Surv. Open File Rep.*, 75–311 pp.

Li, Y. G., P. Chen, E. S. Cochran, J. E. Vidale, and T. Burdette (2006), Seismic evidence for rock damage and healing on the San Andreas fault associated with the 2004 M 6.0 Parkfield earthquake, *Bull. Seismol. Soc. Am.*, *96*, S349–S363.

Lin, J., and R. S. Stein (2004), Stress triggering in thrust and subduction earthquakes and stress interaction between the southern San Andreas and nearby thrust and strike-slip faults, *J. Geophys. Res.*, *109*, B02303, doi:10.1029/2003JB002607.

Lyon-Caen, H., P. Papadimitriou, A. Deschamps, P. Bernard, K. Makropoulos, F. Pacchiani, and G. Patau (2004), First results of the CRLNET seismic network in the western Corinth Rift: Evidence for old-fault reactivation, *CR Geosci.*, *336*, 343–351.

Martini, F., C. J. Bean, G. Saccorotti, F. Viveiros, and N. Wallenstein (2009), Seasonal cycles of seismic velocity variations detected using coda wave interferometry at Fogo volcano, Sao Miguel, Azores, during 2003–2004, *J. Volcanol. Geotherm. Res.*, *181*, 231–246.

McCloskey, J., and S. S. Nalbant (2009), Near-real-time aftershock hazard maps, *Nat. Geosci.*, *2*, 154–155, doi:110.1038/ngeo1449.

Möllhoff, M., and C. J. Bean (2009), Validation of elastic wave measurements of rock fracture compliance using numerical discrete particle simulations, *Geophys. Prospect.*, *57*(5), 883–895, doi:810.1111/j.1365-2478.2008.00749.x.

Nalbant, S. l. S., A. l. Hubert, and G. C. P. King (1998), Stress coupling between earthquakes in northwest Turkey and the north Aegean Sea, *J. Geophys. Res.*, *103*, 24,469–24,486.

Niu, F. L., P. G. Silver, T. M. Daley, X. Cheng, and E. L. Majer (2008), Preseismic velocity changes observed from active source monitoring at the Parkfield SAFOD drill site, *Nature*, *454*, 204–U244.

Pacchiani, F. (2006), Estude sismologique des failles noramles actives du Rift de Corinthe, Ph.D thesis, Université Paris XI, France, 26 September.

Pacchiani, F., and H. Lyon-Caen (2009), Geometry and spatio-temporal evolution of the 2001 Agios Ioanis earthquake swarm (Corinth Rift, Greece), *Geophys. J. Int.*, *180*, 59–72, doi:10.1111/j.1365-246x.2009.04409.x.

Pandolfi, D., C. J. Bean, and G. Saccorotti (2006), Coda wave interferometric detection of seismic velocity changes associated with the 1999 M = 3.6 event at Mt. Vesuvius, *Geophys. Res. Lett.*, *33*, L06306, doi:10.1029/2005GL025355.

Paul, A., M. Campillo, L. Margerin, E. Larose, and A. Derode (2005), Empirical synthesis of time-asymmetrical Green's functions from the correlation of coda waves, *J. Geophys. Res.*, *110*, B08302, doi:10.1029/2004JB003521.

Peng, Z. G., and Y. Ben-Zion (2006), Temporal changes of shallow seismic velocity around the Karadere-Duzce branch of the north Anatolian fault and strong ground motion, *Pure Appl. Geophys.*, *163*, 567–600.

Poupinet, G., W. L. Ellsworth, and J. Frechet (1984), Monitoring velocity variations in the crust using earthquake doublets – An application to the Calaveras Fault, California, *J. Geophys. Res.*, *89*, 5719–5731.

Pyrak-Nolte, L. J., and J. P. Morris (2000), Single fractures under normal stress: The relation between fracture specific stiffness and fluid flow, *Int. J. Rock Mech. Min.*, *37*, 245–262.

Pyrak-Nolte, L. J., L. R. Myer, and N. G. W. Cook (1990), Transmission of Seismic-Waves across Single Natural Fractures, *J. Geophys. Res.*, *95*, 8617–8638.

Rigo, A., H. LyonCaen, R. Armijo, A. Deschamps, D. Hatzfeld, K. Makropoulos, P. Papadimitriou, and I. Kassaras (1996), A microseismic study in the western part of the Gulf of Corinth (Greece): Implications for large-scale normal faulting mechanisms, *Geophys. J. Int.*, *126*, 663–688.

Rubinstein, J. L., and G. C. Beroza (2004), Nonlinear strong ground motion in the M-L 5.4 Chittenden earthquake: Evidence that preexisting damage increases susceptibility to further damage, *Geophys. Res. Lett.*, *31*, L23614, doi:10.1029/2004GL021357.

Sabra, K. G., P. Gershoft, P. Roux, and W. A. Kuperman (2005), Extracting time-domain Green's function estimates from ambient seismic noise, *Geophys. Res. Lett.*, *32*, L03310, doi:10.1029/2004GL021862.

Schaff, D. P., and G. C. Beroza (2004), Coseismic and postseismic velocity changes measured by repeating earthquakes, *J. Geophys. Res.*, *109*, B10302, doi:10.1029/2004JB003011.

Sens-Schönfelder, C., and U. Wegler (2006), Passive image interferometry and seasonal variations of seismic velocities at Merapi Volcano, Indonesia, *Geophys. Res. Lett.*, *33*, L21302, doi:10.1029/2006GL027797.

Silver, P. G., T. M. Daley, F. L. Niu, and E. L. Majer (2007), Active source monitoring of cross-well seismic travel time for stress-induced changes, *Bull. Seismol. Soc. Am.*, *97*, 281–293, doi:210.1785/0120060120.

Snieder, R. (2006), The theory of coda wave interferometry, *Pure Appl. Geophys.*, *163*, 455–473, doi:410.1007/s00024-00005-00026-00026.

Snieder, R., A. Gret, H. Douma, and J. Scales (2002), Coda wave interferometry for estimating nonlinear behavior in seismic velocity, *Science*, *295*, 2253–2255, doi:2210.1126/science.1070015.

Toda, S., R. S. Stein, K. Richards-Dinger, and S. B. Bozkurt (2005), Forecasting the evolution of seismicity in southern California: Animations built on earthquake stress transfer, *J. Geophys. Res.*, *110*, B05S16, doi:10.1029/2004JB003415.

Velasco, A. A., S. Hernandez, T. Parsons, and K. Pankow (2008), Global ubiquity of dynamic earthquake triggering, *Nat. Geosci.*, *1*, 375–379, doi:310.1038/ngeo1204.

Vidale, J. E., and Y. G. Li (2003), Damage to the shallow Landers fault from the nearby Hector Mine earthquake, *Nature*, *421*, 524–526, doi:510.1038/nature01354.

Waldhauser, F., and W. L. Ellsworth (2000), A double-difference earthquake location algorithm: Method and application to the northern Hayward fault, California, *Bull. Seismol. Soc. Am.*, *90*, 1353–1368, doi:1310.1785/0120000006.

Wegler, U., and C. Sens-Schönfelder (2007), Fault zone monitoring with passive image interferometry, *Geophys. J. Int.*, *168*, 1029–1033, doi:1010.1111/j.1365-1246X.2006.03284.x.

Wegler, U., H. Nakahara, C. Sens-Schönfelder, M. Korn, and K. Shiomi (2009), Sudden drop of seismic velocity after the 2004 Mw 6.6 mid-Niigata earthquake, Japan, observed with passive image interferometry, *J. Geophys. Res.*, *114*, B06305, doi:10.1029/2008JB005869.

Worthington, M. H., and R. Lubbe (2007), The scaling of fracture compliance, *Frac. Res.*, *270*, 73–82, 285.

Yamamura, K., O. Sano, H. Utada, Y. Takei, S. Nakao, and Y. Fukao (2003a), Long-term observation of in situ seismic velocity and attenuation, *J. Geophys. Res.*, *108*(B6), 2317, doi:10.1029/2002JB002005.

Yamamura, K., O. Sano, H. Utada, Y. Takei, S. Nakao, and Y. Fukao (2003b), Long-term observation of in situ seismic velocity and attenuation, *J. Geophys. Res.*, *108*(B6), 2317, doi:10.1029/2002JB002005.

Zahradnik, J., J. Jansky, E. Sokos, A. Serpetsidaki, H. Lyon-Caen, and P. Papadimitriou (2004), Modeling the M(L)4.7 main shock of the February–July 2001 earthquake sequence in Aegion, Greece, *J. Seismol.*, *8*, 247–257.

C. J. Bean and L. Cociani, Seismology and Computational Rock Physics Laboratory, School of Geological Sciences, University College Dublin, Belfield, Dublin 4, Ireland. (lorenzo.cociani@ucd.ie)

A. Deschamps, UMR Géoazur, UNS, CNRS, IRD, OCA, 250, rue Albert-Einstein, F-06560 Valbonne, France.

H. Lyon-Caen, Laboratoire de Géologie, Ecole Normale Supérieure, CNRS, 24 rue Lhmond, F-75231 Paris CEDEX 05, France.

F. Pacchiani, Istituto Nazionale di Oceanografia e di Geofisica Sperimentale, Borgo Grotta Gigante, I-34100 Sgonico, Trieste, Italy.